AEE788, a Dual Tyrosine Kinase Receptor Inhibitor, Induces Endothelial Cell Apoptosis in Human Cutaneous Squamous Cell Carcinoma Xenografts in Nude Mice

Young Wook Park,[1] Maher N. Younes,[1] Samar A. Jasser,[1] Orhan G. Yigitbasi,[1] Ge Zhou,[1] Corazon D. Bucana,[2] Benjamin N. Bekele,[3] and Jeffrey N. Myers[1,2]

Departments of [1]Head and Neck Surgery, [2]Cancer Biology, and [3]Biostatistics, University of Texas M.D. Anderson Cancer Center, Houston, Texas

ABSTRACT

Purpose: **We investigated whether concomitant blockade of the epidermal growth factor receptor (EGFR) and vascular endothelial growth factor receptor (VEGFR) signaling pathways by AEE788, a dual inhibitor of EGFR and VEGFR tyrosine kinases, would inhibit the growth of cutaneous squamous cell carcinoma (SCC) cells and human cutaneous cancer xenografts in nude mice.**

Experimental Design: **We examined the effects of AEE788 on the phosphorylation of EGFR and VEGFR-2 in cutaneous SCC cells expressing EGFR and VEGFR-2 and cutaneous SCC cell growth and apoptosis. We assessed the *in vivo* antitumor effects of AEE788 in a xenograft model in nude mice. AEE788 (50 mg/kg) was given orally thrice weekly to mice that had been s.c. injected with Colo16 tumor cells. Mechanisms of *in vivo* AEE788 activity were determined by immunohistochemical analysis.**

Results: **Treatment of cutaneous SCC cells with AEE788 led to dose-dependent inhibition of EGFR and VEGFR-2 phosphorylation, growth inhibition, and induction of apoptosis. In mice treated with AEE788, tumor growth was inhibited by 54% at 21 days after the start of treatment compared with control mice ($P < 0.01$). Immunohistochemical analysis revealed that AEE788 inhibited phosphorylation of EGFR and VEGFR and induced apoptosis of tumor cells and tumor-associated endothelial cells.**

Conclusions: **In addition to inhibiting cutaneous cancer cell growth by blocking EGFR and VEGFR signaling pathways *in vitro*, AEE788 inhibited *in vivo* tumor growth by inducing tumor and endothelial cell apoptosis.**

Received 8/18/04; revised 11/17/04; accepted 12/3/04.
Grant support: National Cancer Institute Head and Neck Specialized Programs of Research Excellence Program grant P50-CA97007-02.
The costs of publication of this article were defrayed in part by the payment of page charges. This article must therefore be hereby marked *advertisement* in accordance with 18 U.S.C. Section 1734 solely to indicate this fact.
Requests for reprints: Jeffrey N. Myers, Department of Head and Neck Surgery, University of Texas M.D. Anderson Cancer Center, 1515 Holcombe Boulevard, Unit 441, Houston, TX 77030-4009. Phone: 713-792-6920; Fax: 713-794-4662; E-mail: jmyers@mdanderson.org.

INTRODUCTION

About 1 million cases of keratinocyte carcinoma are diagnosed annually in the United States (1). Cutaneous squamous cell carcinoma (SCC) accounts for up to 20% of cases of keratinocyte carcinoma (2). The vast number of cases and the morbidity associated with these tumors make the disease a major public health burden (3). Most tumors are surgically excised, but more advanced tumors can recur even after surgery, radiotherapy, or both. Therefore, new treatment strategies are needed.

For this purpose, therapies that target molecules, which are important in maintaining the malignant phenotype, are particularly attractive. In cutaneous SCC, two such targets are growth and angiogenic signaling pathways. Several studies have linked the epidermal growth factor receptor (EGFR) pathway to cutaneous SCC tumorigenesis and progression (4–6), and others have shown that EGFR is associated with poor prognosis in patients with head and neck SCC (7). Tumor angiogenesis is essential to sustaining the malignant phenotype of any tumor. Vascular endothelial growth factor (VEGF) seems to be a major mitogen and survival factor for endothelial cells (8, 9). Studies have shown that higher VEGF expression is associated with progression in cutaneous SCC (10–13) and with decreased overall survival rates in patients with basal cell carcinoma and cutaneous SCC (14).

Based on these findings, several EGFR-targeting agents, such as PKI-166, C-225, ZD1839, and OSI-774, have been developed and tested in mucosal SCC of the head and neck both preclinically (15–17) and clinically (18–21). Previous work has shown that EGFR signaling plays a role in angiogenesis because inhibition of EGFR decreases the production of proangiogenic molecules by tumor cells and inhibits neoangiogenesis (22, 23). Thus, EGFR inhibitors have some antiangiogenic activity as well as direct effects on tumor cell proliferation. Therefore, we reasoned that additional inhibition of VEGF receptor (VEGFR) activity would accentuate the antitumor effects of EGFR inhibitors.

AEE788 (Novartis Pharma AG, Basel, Switzerland), a novel dual inhibitor of EGFR/ErbB2 and VEGFR tyrosine kinases, inhibits growth in several cancer cell lines that overexpress EGFR and exhibits antitumor activity in tumor models of human small cell lung and prostate carcinoma in mice (24). However, the effect of AEE788 on cutaneous SCC has not been reported. Therefore, we investigated the effects of AEE788 on *in vitro* growth of cutaneous SCC cells and *in vivo* growth of human tumor xenografts transplanted into nude mice.

MATERIALS AND METHODS

Cell Lines and Culture Conditions. Three human cutaneous SCC cell lines (Colo16, SRB1, and SRB12) and a skin keratinocyte cell line (HaCaT) were used. All these cells were maintained as monolayer cultures in DMEM supplemented

with 10% fetal bovine serum, sodium pyruvate, nonessential amino acids, L-glutamine, vitamins (Life Technologies, Rockville, MD), and penicillin-streptomycin (Flow Laboratories, Rockville, MD). The cells were incubated in a mixture of 5% CO_2 and 95% air at 37°C.

Chemical Compounds. AEE788 was synthesized and provided by Novartis Pharma. For *in vivo* administration, AEE788 was dissolved in 90% polyethylene glycol 300 plus 10% 1-methyl-2-pyrrolidinone to a concentration of 6.25 mg/mL. Propidium iodide and 3-(4,5-dimethylthiazol-2-yl)-2, 5-diphenyltetrazolium bromide (MTT) were purchased from Sigma Chemical Co. (St. Louis, MO).

Western Blot Analysis. Total cell protein extracts were obtained from Colo16, HaCaT, SRB1, and SRB12 cells. Briefly, the cells were washed with PBS, scraped with lysis buffer [1% Triton X-100, 20 mmol/L Tris-HCl (pH 8.0), 137 mmol/L NaCl, 10% glycerol, 2 mmol/L EDTA, 1 mmol/L phenylmethylsulfonyl fluoride, 20 μmol/L leupeptin, 0.15 units/mL aprotinin, 2 mmol/L sodium orthovanadate], and centrifuged to remove insoluble protein. Samples were diluted in sample buffer [0.5 mmol/L Tris-HCl (pH 6.8), 10% SDS, 1 mol/L DTT, 10% glycerol, 1% bromophenol blue] and boiled.

For Western blotting, protein (100 μg) was electrophoresed on 10% (7.5% for VEGFR-2) SDS-PAGE and transferred to polyvinylidene difluoride membrane. The membranes were blocked with 5% nonfat milk in TBST [0.1% (v/v) Tween 20 in TBS] for 1 hour and incubated overnight with rabbit polyclonal anti-phospho-EGFR (Tyr^{1068}, Cell Signaling Technology, Beverly, MA), anti-phospho-VEGFR-2 (Tyr^{1054}, Biosource International, Camarillo, CA), anti-phospho-Akt (Ser^{473}, Cell Signaling Technology, or anti-phospho-mitogen-activated protein kinase (MAPK; Thr^{202}/Tyr^{204}, Cell Signaling Technology) antibody. The blot was washed with TBST and incubated for 1 hour with horseradish peroxidase–conjugated anti-rabbit IgG (Santa Cruz Biotechnology, Santa Cruz, CA). Immunoreactive proteins were visualized using an enhanced chemiluminescence detection system (Amersham, Inc., Arlington Heights, IL).

After stripping, membranes were reprobed with sheep polyclonal anti-EGFR (Upstate, Lake Placid, NY), mouse monoclonal anti-VEGFR-2 (Santa Cruz Biotechnology), rabbit polyclonal anti-Akt, mouse monoclonal anti-MAPK (p42 MAPK), or anti-β-actin (Sigma Chemical) antibody, which served as protein and loading controls.

To determine whether *in vitro* treatment of Colo16 cells with AEE788 can inhibit tyrosine phosphorylation of EGFR, VEGFR-2, Akt, and MAPK, serum-starved Colo16 cells were treated with AEE788 (0.001-2 μmol/L) and DMSO for controls for 1 hour and incubated with or without 40 ng/mL EGF for 15 minutes. Cell protein extracts were obtained and Western blotting was done as described above.

***In vitro* Cytotoxicity Assay.** In all of the assays, 1,000 tumor cells were seeded into 96-well plates in complete medium and allowed to attach for 24 hours. The cultures were re-fed with medium with 2% serum. After 24 hours, cells were treated with different concentrations of AEE788 (negative control with DMSO alone) for 72 hours. The metabolically active cells were determined by MTT assay (25). After a 2-hour incubation in medium containing 0.42 mg/mL MTT, the cells were lysed in 100 μL DMSO. The conversion of MTT to formazan was measured using a MR-5000 six-well microtiter plate reader at an absorbance of 570 nm (Dynatech, Inc., Chantilly, VA).

Apoptosis Assays

Flow Cytometric Analysis. Colo16, SRB1, and SRB12 cells (2×10^5 per well) were plated into six-well plates (Costar, Cambridge, MA). After cell attachment, the cultures were re-fed with medium with 2% serum for 24 hours and then treated with AEE788 at different concentrations. After 48 hours, both adherent and detached cells were harvested, washed with PBS, and resuspended in propidium iodide (50 μg/mL) in 0.1% sodium citrate for 20 minutes. Flow cytometric analysis was done and the percentage of apoptotic cells was calculated by gating the hypodiploid region on the DNA content histogram using Lysys software (Becton Dickinson, Franklin Lakes, NJ). The sub-G_0/G_1 fraction was used as a measure of the percentage of apoptotic cells (26).

DNA Isolation and Electrophoresis. Serum-starved Colo16 cells were grown in the absence or presence of AEE788 at concentration to achieve IC_{50}. After 12 and 24 hours, floating and attached cells were collected and lysed. Soluble DNA was extracted with phenol/chloroform, precipitated in ethanol, and electrophoresed on a 1.8% agarose gel. The gels were then stained with ethidium bromide and photographed in the dark using UV illumination.

Western Blotting. After 24-hour treatment of Colo16 cells with AEE788 (IC_{50}), cell protein extracts were obtained. Protein (50 μg) was electrophoresed through a polyacrylamide gel and transferred to a polyvinylidene difluoride membrane. The membranes were incubated with anti–poly(ADP-ribose) polymerase (clone C2-10, Trevigen, Gaithersburg, MD), anti-caspase-3 (PharMingen, San Diego, CA), anti-phospho-Bad (Ser^{136}, Cell Signaling Technology), anti-Bcl-2 (DAKO A/S, Copenhagen, Denmark), or anti-Bax (Santa Cruz Biotechnology) antibody. Horseradish peroxidase–conjugated anti-rabbit or anti-mouse IgG was used as the secondary antibody. β-actin was used to confirm protein levels.

Evaluation of Epidermal Growth Factor Receptor Mutations. To determine whether the SCC cell lines harbor EGFR mutations that might render them more sensitive to AEE788, PCR was used to amplify exons 18, 19, and 21 from the human *EGFR* gene using genomic DNA isolated from Colo16, SRB1, and SRB12 cells. The sequences of PCR primers are the same as the ones reported previously (27). PCR amplicons were purified using QIAquick PCR purification kit (Qiagen, Valencia, CA) and sent for sequencing. The sequencing results were then blasted and compared with the wild-type *EGFR* sequence from the Genbank.

Evaluation of Vascular Endothelial Growth Factor Secretion. To verify the effect of AEE788 on the production of VEGF by the cutaneous SCC cell lines, Colo16, SRB1, and SRB12 cells (1,000 cells per 38-mm^2 well) were plated into 96-well plates in 200 μL DMEM supplemented with 10% fetal bovine serum. After cell attachment, the cultures were re-fed with medium with 2% serum for 24 hours and then treated with AEE788 (IC_{50}) for each cell line for 72 hours. DMEM served as control. The concentration of VEGF in the conditioned medium obtained from each cell line was measured using Quantikine

ELISA kits (R&D Systems, Minneapolis, MN) according to the manufacturer's instructions. Results were normalized for the number of VEGF-producing cells and reported in picograms of growth factor per total number of cells.

Animals and *In vivo* Assay. Male nude mice were purchased from the National Cancer Institute-Frederic Cancer Research and Development Center (Frederick, MD). Mice were maintained in a pathogen-free environment and used in accordance with the Animal Care and Use Guidelines of the University of Texas M.D. Anderson Cancer Center. Mice used for this study were 8 to 10 weeks old.

In HBSS (100 μL), 4×10^5 Colo16 cells per mouse were injected s.c. into the dorsal flank area. Eleven days after injection of the tumor cells, tumor nodules were palpable. Mice were randomized into two groups ($n = 10$). Mice in group 1 were treated with 50 mg/kg AEE788, which had been predetermined in our laboratory, given by oral gavage thrice a week, and mice in group 2 received the same vehicle used for administration of AEE788 (control). Treatments continued for 3 weeks. Tumor size and body weight were measured twice a week. Tumor volume was calculated using the formula: (length) (width^2) π / 6 and expressed in cubic millimeters.

To determine overall survival of mice, we repeated the therapy experiment. Mice were s.c. implanted with Colo16 cells (4×10^5). On day 11, mice were randomized ($n = 10$) to the two treatment groups as described above. Mice were sacrificed using CO_2 when they had lost >25% of their initial body weight.

After mice were euthanized, specimens of xenograft tumors were obtained. For immunohistochemical and routine H&E staining, one part of the tumor tissue was fixed in formalin and embedded in paraffin. Another part was embedded in OCT compound (Miles, Inc., Elkhart, IN), rapidly frozen in liquid nitrogen, and stored at −70°C.

Reagents for Immunohistochemical and Terminal Deoxynucleotidyl Transferase–Mediated dUTP Nick End Labeling Assays. The following antibodies were used for immunohistochemistry: polyclonal rabbit anti-EGFR (Santa Cruz Biotechnology) and anti-phospho-EGFR (Biosource International); polyclonal rabbit anti-VEGFR-2 and anti-phospho-VEGFR-2 (Oncogene, Cambridge, MA); polyclonal rabbit anti-Akt and anti-phospho-Akt; polyclonal rabbit anti-MAPK (Zymed Laboratories, South San Francisco, CA) and anti-phospho-MAPK; mouse anti-proliferating cell nuclear antigen (PCNA) clone PC-10 (DAKO); monoclonal rat anti-CD31/platelet-endothelial cell adhesion molecule-1 (PharMingen); polyclonal rabbit anti-VEGF (Santa Cruz Biotechnology); polyclonal rabbit anti-interleukin (IL)-8 (Biosource International);polyclonal rabbit anti–basic fibroblast growth factor (bFGF; Sigma Chemical); peroxidase-conjugated goat anti-rabbit IgG (Jackson ImmunoResearch Laboratories, West Grove, PA); peroxidase-conjugated rat anti-mouse IgG2a (Serotec, Harlan Bioproducts for Science, Inc., Indianapolis, IN); peroxidase-conjugated goat anti-rat IgG1 (Jackson ImmunoResearch Laboratories); and Alexa Fluor 594–conjugated goat anti-rat IgG and Alexa Fluor 594–conjugated goat anti-rabbit IgG (Molecular Probes, Eugene, OR).

Terminal deoxynucleotidyl transferase–mediated dUTP nick end labeling (TUNEL) assay was done using a commercial apoptosis detection kit (Promega Corp., Madison, WI).

Single-Label Immunofluorescence for Epidermal Growth Factor Receptor/Activated Epidermal Growth Factor Receptor, Vascular Endothelial Growth Factor Receptor/Activated Vascular Endothelial Growth Factor Receptor, Akt/Activated Akt, and Mitogen-Activated Protein Kinase/Activated Mitogen-Activated Protein Kinase. Frozen tissues were sectioned at 8 to 10 μm, mounted on positively charged Plus slides (Fisher Scientific, Houston, TX), and air-dried for 30 minutes. Sections were fixed in cold acetone (5 minutes), 1:1 (v/v) acetone/chloroform (5 minutes), and acetone (5 minutes) and then washed with PBS. Immunofluorescent procedures were done as described previously (28). Dilutions of primary antibodies were as follows: EGFR 1:200, phospho-EGFR 1:500, VEGFR-2 1:200, phospho-VEGFR-2 1:100, Akt 1:100, phospho-Akt 1:100, MAPK 1:100, and phospho-MAPK 1:100. A positive reaction was detected by indirect immunofluorescence.

Immunohistochemical Determination of Proliferating Cell Nuclear Antigen, Vascular Endothelial Growth Factor, Interleukin-8, Basic Fibroblast Growth Factor, and CD31/Platelet-Endothelial Cell Adhesion Molecule-1. Paraffin-embedded tissues were sectioned at 4 to 6 μm and mounted on positively charged Superfrost slides and dried overnight. Sections were deparaffinized in xylene, dehydrated with a graded series of alcohol, and rehydrated in PBS. For antigen retrieval, sections for PCNA were microwaved for 5 minutes and sections for VEGF, IL-8, and bFGF were incubated with pepsin (Biomeda, Foster City, CA) for 20 minutes at 37°C. Frozen tissues were used for detection of CD31/platelet-endothelial cell adhesion molecule-1.

Dilutions of primary antibodies were as follows: PCNA 1:100, VEGF 1:500, IL-8 1:50, bFGF 1:1,000, and CD31/platelet-endothelial cell adhesion molecule-1 1:400. Indirect peroxidase technique was used and a positive reaction was visualized by incubating the slides with stable 3,3′-diaminobenzidine (Research Genetics, Huntsville, AL) for 5 to 10 minutes. The sections were rinsed with distilled water, counterstained with Gill's hematoxylin (Sigma Chemical), and mounted with Universal Mount (Research Genetics). Stained sections were examined in a Nikon Microphot-FX microscope (Nikon, Inc., Garden City, NY) equipped with a three-chip CCD color video camera (model DXC990, Sony Corp., Tokyo, Japan).

Immunofluorescence Double Staining for CD31/Terminal Deoxynucleotidyl Transferase–Mediated dUTP Nick End Labeling, CD31/Activated Epidermal Growth Factor Receptor, and CD31/Activated Vascular Endothelial Growth Factor Receptor. For TUNEL and double immunofluorescence assays, frozen tissues were used. After fixation with acetone, the samples were washed with PBS, incubated with protein blocking solution containing 5% normal horse serum and 1% normal goat serum in PBS for 20 minutes, and then incubated with a 1:400 dilution of rat anti-mouse CD31 monoclonal antibody overnight at 4°C. After washing with PBS, the slides were incubated with a 1:600 dilution of secondary goat anti-rat antibody conjugated to Alexa Fluor 594 (red) for 1 hour in the dark.

TUNEL assay was done using an apoptosis detection kit with the following modifications. Samples were fixed with 4% paraformaldehyde for 10 minutes, washed twice with PBS for

5 minutes, and then incubated with 0.2% Triton X-100 for 15 minutes. After two 5-minute washes with PBS, the samples were incubated with equilibration buffer for 10 minutes. The equilibration buffer was drained, and the reaction buffer containing 44 μL equilibration buffer, 5 μL nucleotide mix, and 1 μL terminal deoxynucleotidyl transferase (Promega kit) was added to the sections and incubated in a humid atmosphere at 37°C for 1 hour, avoiding exposure to light. The reaction was terminated by immersing the samples in 2× SSC for 15 minutes. Samples were then washed with PBS to remove unincorporated fluorescein-dUTP.

Immunofluorescence double staining was done by staining frozen samples with CD31. The samples were then incubated with primary antibodies for anti-phospho-EGFR (1:50) and anti-phospho-VEGFR (1:400) overnight at 4°C. After washing with PBS, the samples were incubated with Alexa Fluor 488 (green)–conjugated secondary antibody for 1 hour at room temperature. To identify the cell nuclei, the samples were incubated with 1 μg/mL Hoechst dye (Hoechst, Warrington, PA) for 2 minutes. Immunofluorescence microscopy was done in a Nikon Microphot-FX equipped with a HBO 100 mercury lamp, narrow bandpass filters to individually select for green, red, and blue fluorescence (Chroma Technology Corp., Brattleboro, VT). Images were captured using a cooled CCD Hamamatsu 5810 camera (Hamamatsu Corp., Bridgewater, NJ) and Optimas Image Analysis software (Media Cybernetics, Silver Spring, MD). Photomontages were prepared using Adobe Photoshop software (Adobe Systems, Inc., San Jose, CA).

Quantification of Proliferating Cell Nuclear Antigen, Microvessel Density, Absorbance, and Apoptotic Tumor and Endothelial Cells. For quantification analysis, five slides were prepared for each group and two areas were selected in each slide. To quantify the PCNA and TUNEL expression, the number of positively stained cells and total cells were also counted in 10 random 0.159-mm^2 fields of tumor area at ×100 magnification. The percentages of positively stained cells among the total number of cells were calculated and compared.

To quantify microvessel density (MVD), areas containing the higher number of tumor-associated blood vessels were identified by scanning the tumor sections at low microscopic power (×40). The vessels that were completely stained with anti-CD31 antibodies were then counted in 10 random 0.159-mm^2 fields at ×100 magnification (29).

For the quantification of immunohistochemical intensity, the absorbance of 100 VEGF-, IL-8-, and bFGF-positive cells in 10 random 0.039-mm^2 fields at ×200 magnification taken from treated tumor tissues was measured using the Optimas Image Analysis software (22). The samples were not counterstained so that the absorbance would be attributable solely to the product of the immunohistochemical reaction. VEGF, IL-8, and bFGF cytoplasmic immunoreactivity was evaluated by computer-assisted image analysis and expressed as a density value.

Quantification of apoptotic endothelial cells was expressed as the average of the ratios of apoptotic endothelial cells to the total number of endothelial cells in 10 random 0.011-mm^2 fields at ×400 magnification.

Statistical Analysis. We calculated the dose and apoptosis rate using a Loess smoother. We also calculated 95% confidence intervals for the IC_{50} values using a parametric bootstrap methodology. For *in vivo* study, on each day of treatment, the Wilcoxon's rank sum test was used to test for any difference in the mean tumor volume and body weight between treatment and control groups. To statistically model treatment, time, and treatment-by-time interactions on mouse tumor volume and body weight over the treatment period, a generalized linear mixed model was used. Survival was analyzed using the Kaplan-Meier method and compared using the log-rank test. Quantitative analysis for the immunohistochemical expression of PCNA, TUNEL, CD31, absorbance, and CD31/TUNEL were compared by unpaired Student's *t* test. For all analysis, $P < 0.05$ was considered statistically significant.

RESULTS

Cutaneous Squamous Cell Carcinoma Cell Lines Express Epidermal Growth Factor Receptor and Vascular Endothelial Growth Factor Receptor-2. The human cutaneous SCC cells expressed high levels of phospho-EGFR and phospho-VEGFR-2 as well as phospho-Akt and phospho-MAPK that are known to signal downstream of EGFR (Fig. 1*A*). However, the HaCaT cells did not express phospho-EGFR and phospho-VEGFR-2. These data reveal that the EGFR and VEGFR-2 are present and autophosphorylated in human cutaneous SCC cell lines.

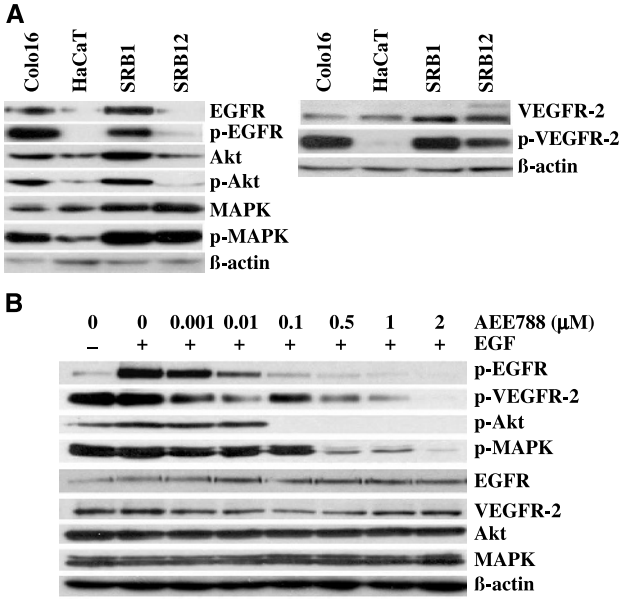

Fig. 1 Effect of AEE788 on protein expression and phosphorylation level in human cutaneous SCC cell lines. *A,* whole cell lysates were prepared from subconfluent Colo16, HaCaT, SRB1, and SRB12 cells. Proteins were resolved on SDS-PAGE gels, transferred to polyvinylidene difluoride membrane, and analyzed by Western blotting using anti-phospho-EGFR (Tyr^{1068}), anti-phospho-VEGFR-2 (Tyr^{1054}), anti-phospho-Akt (Ser^{473}), or anti-phospho-MAPK (Thr^{202}/Tyr^{204}) antibody. Membranes were reprobed with anti-EGFR, anti-VEGFR-2, anti-Akt, anti-MAPK, or β-actin as protein and loading controls. *B,* serum-starved Colo16 cells were treated with AEE788 (0-2 μmol/L) for 1 hour and then incubated without or with 40 ng/mL EGF. After cell protein extracts were obtained, Western blotting was done. Each assay was done in triplicate independently with similar results.

Inhibition of Epidermal Growth Factor Receptor, Vascular Endothelial Growth Factor Receptor-2, Akt, and Mitogen-Activated Protein Kinase Phosphorylation. Colo16 cells, which express high levels of phospho-EGFR and phospho-VEGFR-2, were incubated with AEE788 for 1 hour followed by a 15-minute incubation with EGF. The phosphorylation of EGFR, VEGFR-2, Akt, and MAPK of treated cells was inhibited in a dose-dependent manner. The phospho-EGFR and phospho-Akt were completely inhibited at 0.1 μmol/L AEE788 and the phospho-VEGFR-2 and phospho-MAPK were successfully inhibited at 2 μmol/L AEE788. The total levels of EGFR, VEGFR-2, Akt, and MAPK remained unchanged (Fig. 1*B*).

Inhibition of Cell Proliferation. We determined the *in vitro* effects of AEE788 on the growth of human cutaneous SCC cells by incubating Colo16, SRB1, and SRB12 cells in medium containing AEE788 for 3 days and by performing MTT assays. AEE788 inhibited the proliferation of all tested cell lines in a dose-dependent manner (Fig. 2*A*). IC_{50} values of AEE788 were for 0.89 μmol/L for Colo16, 0.21 μmol/L for SRB1, and 0.96 μmol/L for SRB12 cells.

Induction of Apoptosis. Colo16, SRB1, and SRB12 cells were treated *in vitro* with AEE788 and evaluated for apoptosis using propidium iodide and flow cytometric analysis. AEE788 induced apoptosis of the cutaneous SCC cells in a dose-dependent manner (Fig. 2*B*). Apoptosis in 50% of cells was induced at the concentration of AEE788 of 6.75 μmol/L for Colo16, 4.41 μmol/L for SRB1, and 1.6 μmol/L for SRB12 cells.

To determine the mechanism of the apoptosis induced by AEE788, characteristics of apoptosis and the expression level of apoptosis-related proteins were evaluated in Colo16 cells treated with the absence or presence of AEE788. Internucleosomal cleavage of DNA to form a DNA ladder was observed in the Colo16 cells treated with AEE788 for 12 hours (Fig. 2*C*). The control did not cause internucleosomal cleavage of DNA. Poly(ADP-ribose) polymerase (116 kDa) was cleaved, yielding a characteristic 85-kDa fragment in the presence of AEE788. In addition, AEE788 caused activation of caspase-3 (Fig. 2*D*). These results supported the hypothesis that AEE788 increased cell death by inducing apoptosis. For Bcl-2 family proteins, AEE788 had no significant effect on the apoptotic suppressor protein Bcl-2 and the proapoptotic protein Bax. In contrast, the phosphorylation of Bad was inhibited by AEE788 treatment, indicating translocation of Bad to the mitochondria and its activation causing cell death.

PCR Analysis Shows No Epidermal Growth Factor Receptor Mutations. Sequence analysis revealed no mutations

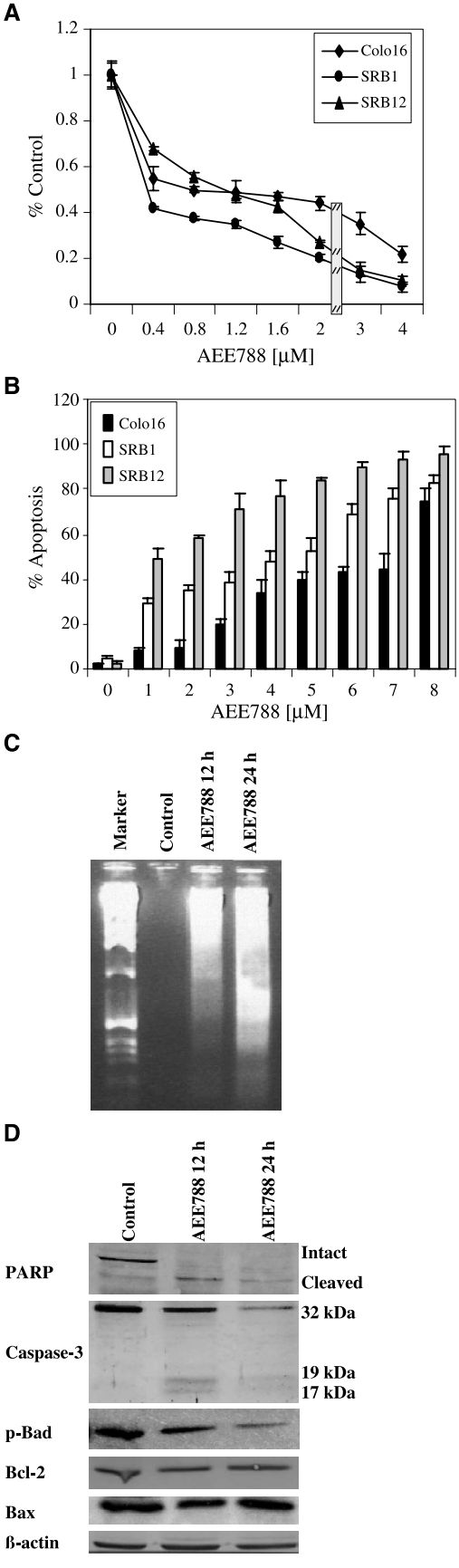

Fig. 2 *In vitro* effects of AEE788 on cell proliferation and apoptosis induction in human cutaneous SCC cells. *A,* cultured cutaneous SCC cells were treated with AEE788 (0-4 μmol/L). Effect on cell growth was measured by MTT assay. Points, mean of triplicate experiments; bars, SD. *B,* cultured cutaneous SCC cells were treated with AEE788 (0-8 μmol/L). Effect on the proportion of apoptosis was determined by flow cytometric assay. Columns, mean of triplicate experiments; bars, SD. *C,* Colo16 cells were treated for 24 hours with AEE788 (0.9 μmol/L) and then were harvested and analyzed by the DNA ladder formation. *D,* Western blotting for poly(ADP-ribose) polymerase (*PARP*), caspase-3, phospho-Bad, Bcl-2, and Bax levels. β-Actin was used as loading control. Each assay was done twice independently with similar results.

in exons 18, 19, and 21 of the *EGFR* gene in Colo16, SRB1, and SRB12 cell lines (data not shown).

Inhibition of Tumor Growth *In vivo* and Prolongation of Animal Survival. To assess the effects of AEE788 on *in vivo* tumor growth, we injected Colo16 cells s.c. into nude mice. All mice were killed on day 21 after the start of treatment because mice in control group had become moribund owing to the increased tumor burden. As shown in Table 1 and Fig. 3*A*, the median xenograft tumor volume of the AEE788-treated mice was significantly lower than that of the control mice ($P < 0.001$ at day 18; $P < 0.01$ at day 21). Treatment with AEE788 was well tolerated as determined by maintenance of body weight (Table 1).

The effect of the treatments on overall survival was determined by a separate study. Compared with the control group, mice treated with AEE788 had a significantly higher survival time ($P < 0.001$; Fig. 3*B*).

***In vivo* Inhibition of Epidermal Growth Factor Receptor, Vascular Endothelial Growth Factor Receptor, Akt, and Mitogen-Activated Protein Kinase Expression and Increase in Tumor and Endothelial Cell Apoptosis.** To evaluate the mechanisms of AEE788 activity *in vivo*, the Colo16 tumors were subjected to immunohistochemical analyses for markers of survival, proliferation, and cell death. Immunofluorescence analysis revealed that the levels of EGFR, VEGFR, Akt, and MAPK expressed by tumors were similar between treatment and control groups. However, activated forms of those kinases were expressed in the treatment group and rarely expressed in the control group (Fig. 4*A*), thus confirming that AEE788 treatment inhibits the phosphorylation of EGFR, VEGFR, Akt, and MAPK *in vivo*.

We evaluated cellular proliferation and apoptosis using anti-PCNA antibody and the TUNEL method, respectively. In the control group, the mean ± SD percentage of PCNA-positive cells was 78.8 ± 6.2. AEE788 treatment significantly reduced the percentage ($P < 0.001$) with a mean ± SD of 26.3 ± 13.8 (Table 2). TUNEL assay revealed that the apoptotic fraction in the tumor specimens was greater for mice treated with AEE788 than for the control group (Fig. 4*B*). The mean ± SD percentage of TUNEL-positive cells in control mice was 1.3 ± 0.8 compared with 12.1 ± 4.1 in AEE788-treated mice and the difference was highly significant ($P < 0.001$).

Table 1 Effects of AEE788 on tumor volume and body weight in nude mice bearing human cutaneous SCC xenografts

	Treatment group*	
Variable	Control (n = 10)	AEE788 (n = 10)
Tumor volume (mm³)		
Median	2,150	1,000†
Range	1,910-2,339	499-1,365
Body weight (g)		
Median	21.9	26.2‡
Range	21.2-24.4	21.8-28.9

*Colo16 human cutaneous SCC cells (4×10^5) were injected s.c. into the flank of nude mice. Eleven days later, mice were randomized for treatment thrice weekly by oral gavage with either AEE788 (50 mg/kg) or the vehicle for AEE788 (control). All mice were killed on day 21 after the start of treatment.

†$P < 0.01$ compared with control (Wilcoxon's rank sum test).

‡$P < 0.05$ compared with control (Wilcoxon's rank sum test).

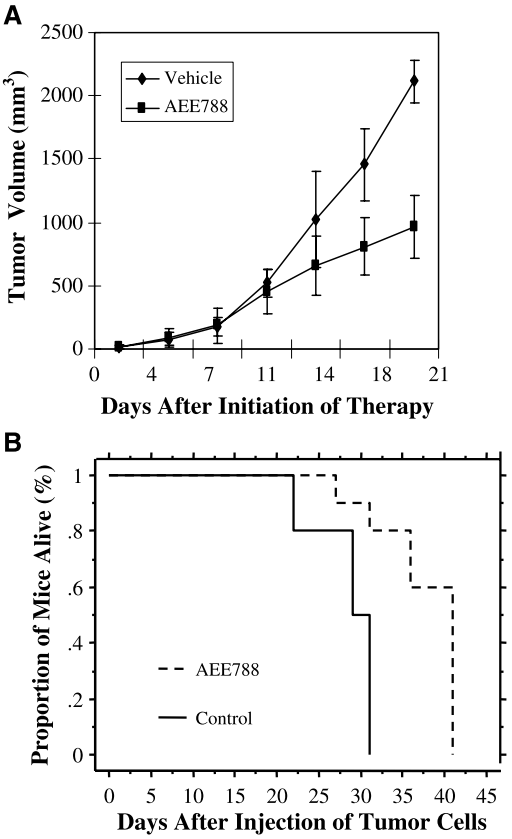

Fig. 3 *In vivo* effects of AEE788 on tumor growth and survival time. Colo16 cells were injected into the dorsal flank of nude mice. After tumor nodules had developed, mice were treated orally either with AEE788 at a dosage of 50 mg/kg thrice a week or with the same vehicle only (control). *A,* tumors were measured twice a week. Points, mean tumor volume; bars, SD. *B,* animals were killed when they had lost >25% of their initial body weight. Survival analysis was computed using the Kaplan-Meier method.

MVD was measured by staining the tumor specimen with antibodies against CD31. AEE788 decreased MVD from 11 ± 3 in control tumors to 4 ± 1 in tumors from mice in the AEE788-treated group (Table 2; $P < 0.001$). Treatment with AEE788 resulted in the decreased expression of bFGF as determined by quantitative analysis ($P < 0.01$). There was no difference in the expression of VEGF and IL-8. These *in vivo* results were supported by an ELISA assay of culture supernatants for VEGF. Our analysis of VEGF secretion into the conditioned medium revealed that, after treatment with AEE788, VEGF was decreased in SRB1 and SRB12 cells but slightly increased in Colo16 cells (data not shown).

Finally, we determined whether tumor-associated endothelial cells express the functional EGFR and whether AEE788 inhibits the function or induces apoptosis of tumor endothelial cells. Endothelial cells of tumors expressed phospho-EGFR as confirmed by the double staining with CD31/activated EGFR. Tumor tissues from the AEE788-treated group did not show any fluorescent yellow signals, thus demonstrating that AEE788 treatment inhibited the phosphorylation of EGFR in the endothelial cells. AEE788 also inhibited the phosphorylation of VEGFR as confirmed

by CD31/activated VEGFR double staining. CD31/TUNEL double labeling revealed that many endothelial cells in tumors treated with AEE788 were undergoing apoptosis (Fig. 4*C*). The percentage of apoptotic endothelial cells was significantly higher in AEE788-treated tumors compared with control tumors (Table 2; $P < 0.001$).

DISCUSSION

The major finding of this study is that AEE788 inhibits cutaneous cancer cell growth *in vitro* by blocking EGFR, VEGFR-2, and their important downstream mediators, Akt and MAPK signaling pathways (30). Furthermore, AEE788 inhibits *in vivo* tumor growth through induction of tumor and endothelial cell apoptosis.

Targeted molecular therapy offers a direct approach for the blockade of growth factor receptor signals governing tumor cell growth and angiogenesis. Recently, dual inhibitors of two receptor tyrosine kinases have emerged to improve the efficacy of single-targeted tyrosine kinase inhibitors (TKI). In the present study, we had selected human cutaneous SCC cell lines and profiled the expression of target proteins of AEE788, which is a dual TKI of EGFR and VEGFR. Our results showed that cutaneous SCC cells express phospho-EGFR and phospho-VEGFR-2. These results are consistent with a report describing the expression of EGFR family members in cutaneous SCC cell lines (31). We also showed that AEE788 can inhibit the phosphorylation of EGFR, VEGFR-2, Akt, and MAPK in Colo16 cells at concentrations between 0.001 and 2 μmol/L, which are well below those reported to be achievable *in vivo* (3.73 ± 0.3 μmol/L) in mice given a single oral dose of 100 mg/kg AEE788 (24).

In the present study, AEE788 inhibited cellular proliferation and induced apoptosis in the cutaneous cancer cell lines. After 24-hour treatment with AEE788 (0.9 μmol/L), evidence for induction of apoptosis was clearly documented by DNA ladder, poly(ADP-ribose) polymerase cleavage, and activation of caspase-3. Akt has been shown to promote cell survival via its ability to phosphorylate Bad at Ser^{136}, which is a proapoptotic member of the Bcl-2 family (32). Our Western blot and apoptosis assays suggest that inhibition of EGFR by AEE788 decreased activity of the survival protein Akt and subsequently prevented downstream phosphorylation of Bad, with concomitant apoptosis of the cutaneous SCC cells. No effects on Bcl-2 levels or Bax expression were noted with AEE788 treatment.

Moreover, when AEE788 was given orally to nude mice bearing Colo16 tumor xenografts, it reduced the growth of the primary tumors by 46%. AEE788 therapy also significantly prolonged survival. Recently, the clinical responsiveness to EGFR inhibitor in human lung cancer is closely related with

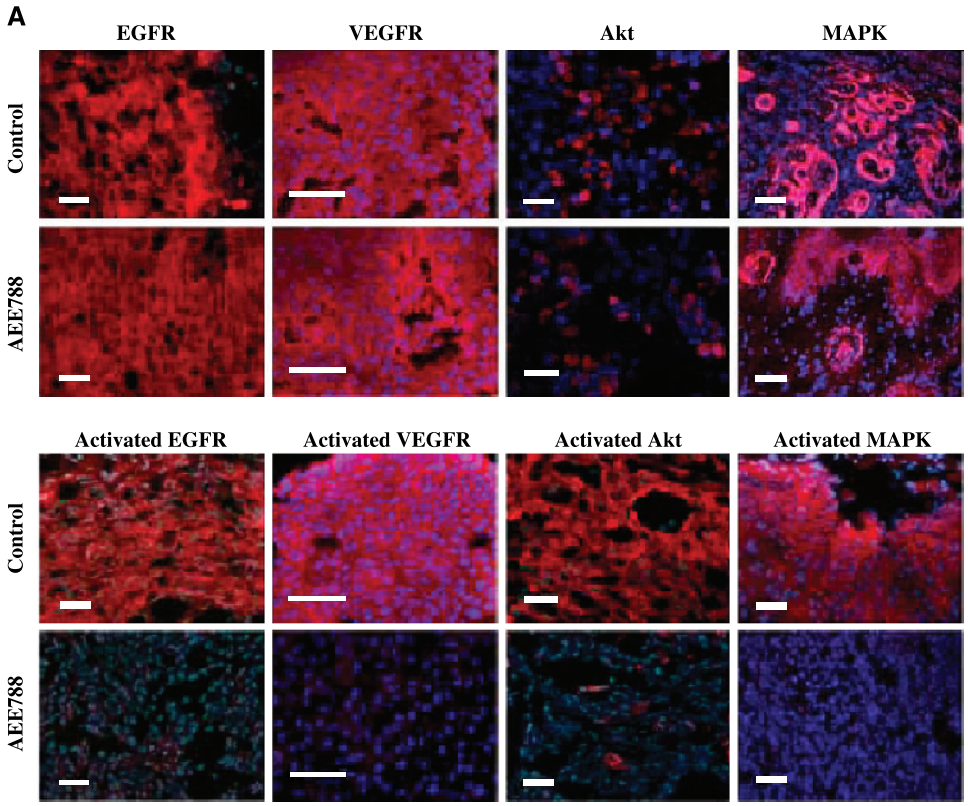

Fig. 4 Immunohistochemical analysis of Colo16 s.c. tumors. Eleven days after injection of Colo16 cells (4×10^5 per mouse), groups of mice ($n = 10$) received either AEE788 at a dosage of 50 mg/kg thrice a week or the same vehicle only (control). Tumors were harvested and processed for immunohistochemical analysis 21 days after treatment. *A,* tumors from the two treatment groups expressed similar levels of EGFR, VEGFR, Akt, and MAPK. In contrast, tumor cells from mice treated with AEE788 showed decreased phosphorylated (indicated as "activated") activity of EGFR, VEGFR, Akt, and MAPK. Each assay was done twice independently with similar results. Bar, 100 μm.

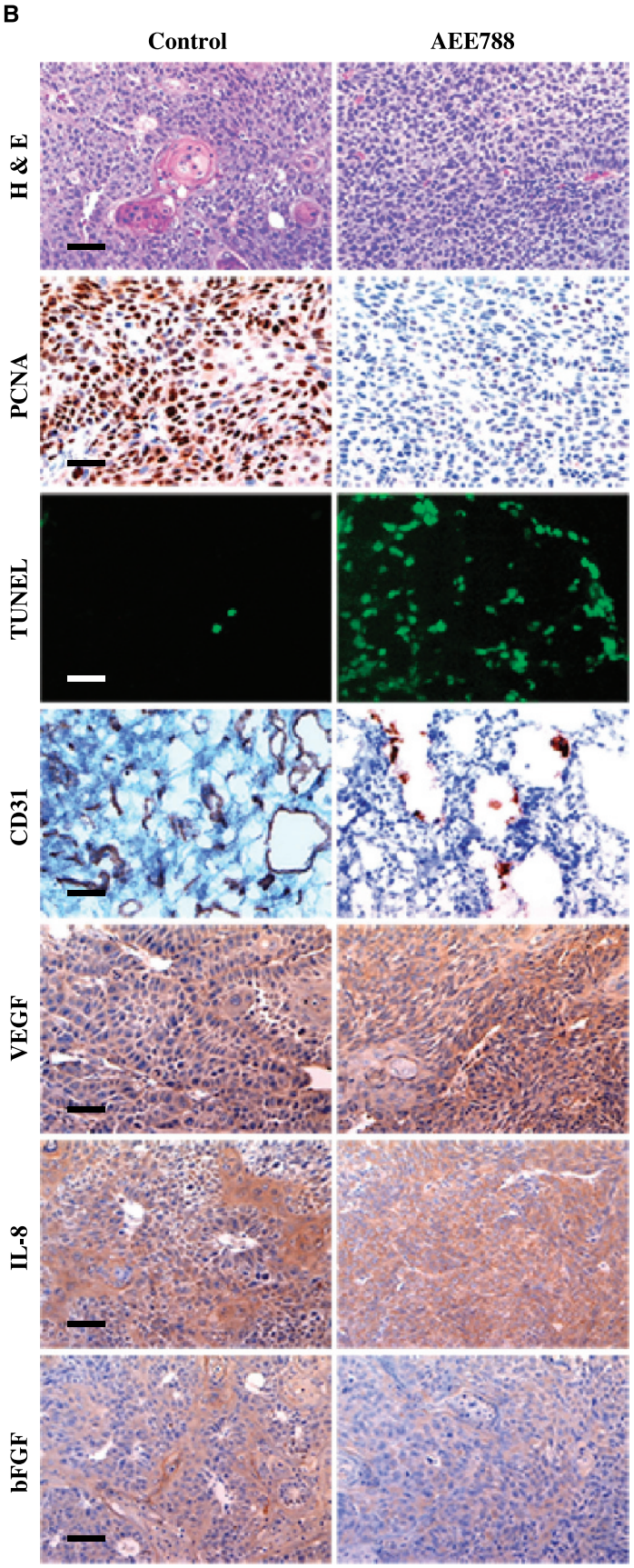

Fig. 4 Continued B, sections were stained with H&E and immunostained for expression of PCNA (a marker of cell proliferation), TUNEL (a marker of cell death), CD31 (an endothelial cell marker), and VEGF, IL-8, and bFGF (all angiogenic factors). Compared with tumors from the control mice, tumors from mice treated with AEE788 showed a decreased number of PCNA-positive cells, an increased number of TUNEL-positive cells, decreased MVD, and decreased expression of bFGF but showed no differences in expression of VEGF and IL-8. Bar, 100 μm.

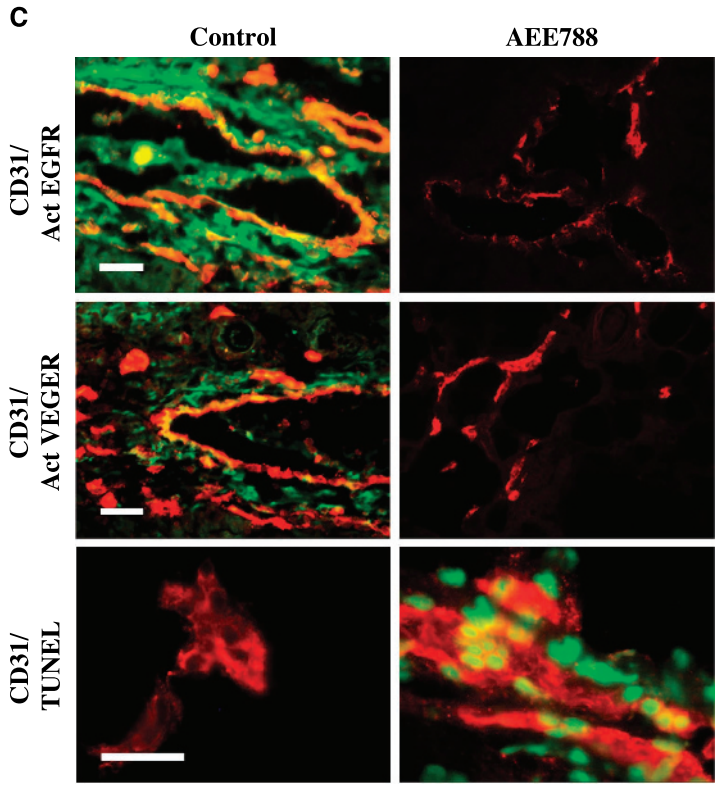

Fig. 4 Continued C, immunofluorescence double staining for CD31 (*red*) plus activated EGFR (*Act EGFR*), activated VEGFR (*Act VEGFR*), or TUNEL (*green*) was done. Endothelial cells within the tumors also expressed activated EGFR (*yellow*). Treatment of mice with AEE788 inhibited phosphorylation of EGFR and VEGFR in the tumor-associated endothelial cells. Representative results of CD31/TUNEL staining. Bar, 50 μm.

specific mutations in exons 18, 19, and 21 of the *EGFR* gene. Such mutations led to increased growth factor signaling and conferred susceptibility to inhibition by gefitinib (27). Our analysis revealed no mutations in exons 18,19, and 21 of the *EGFR* gene in Colo16, SRB1, and SRB12 cells. Our study showed that AEE788 had antiproliferative and cytotoxic effects on cutaneous SCC cells, which had no EGFR mutations. Detailed immunohistochemical analyses showed that activated EGFR and VEGFR-2 were down-regulated in lesions from mice treated with AEE788. Moreover, downstream signaling molecules (Akt and MAPK) of the EGFR pathway, which may play an essential role in the growth of tumors and their response to targeted agents, showed decreased phosphorylation in response to AEE788. This effect was accompanied by a significant decrease in MVD.

VEGF, IL-8, and bFGF are major angiogenic mediators in most epithelial tumors. In cutaneous SCC, VEGF is a marker of tumor invasion and metastasis (33) and altered bFGF expression is common (34). Some studies have shown a direct correlation between VEGF expression and tumor neovascularization as measured by MVD (35, 36). However, this relationship between MVD and increased expression of VEGF has not been detected generally in human malignancies. In our analysis, oral administration of AEE788 significantly decreased bFGF expression but did not affect the protein expression of VEGF and IL-8. Our data suggest that the decrease in MVD was attributable to a decrease in the production of bFGF from the tumor cells as well as to the direct blockade of VEGFR on endothelial cells by use of the dual inhibitor. In other studies, the levels of expression of VEGF, IL-8, and bFGF were reported to be decreased (22, 37) or unchanged (38) immunohistochemically after mice that had been xenografted with human renal (22), pancreatic (37), or prostate (38) cancer cells had been treated with the EGFR TKI (PKI-166). The difference in these results might be attributable to cell type specificity or different model systems used in the studies.

Our double immunofluorescence of endothelial cells revealed that many tumor-associated endothelial cells underwent apoptosis after treatment with AEE788. In a recent study of SU5416, a TKI for Flk-1/KDR, blockade of the VEGFR signaling pathway induced increased tumor cell and endothelial cell apoptosis in a mouse colon cancer model (39). Other studies have shown that endothelial cells of many lesions that produce high levels of EGF express EGFR and activated EGFR (40–42). These results confirm that increased apoptosis of endothelial cells in the present study is attributable to blockade of not only VEGFR signaling but also EGFR signaling on the tumor-associated endothelial cells. Similar results have been reported in previous studies, which have shown that blockade of EGFR signaling by a TKI leads to apoptosis of tumor-associated endothelial cells (43, 44). Together, our data suggest that AEE788 can inhibit the tumor growth of cutaneous SCC by blocking the EGFR signaling pathway in tumor cells and by blocking the EGFR and VEGFR signaling pathways in tumor-associated endothelial cells.

Studies to date have indicated that the *in vivo* efficacy of TKIs may be enhanced by combining them with other targeted agents, chemotherapy, or radiotherapy (45–47). However, the encouraging response rates achieved using ZD1839 and OSI-774 as single agents in non–small cell lung carcinoma (48, 49) provide support for the use of anti-EGFR agents alone. Our experimental results clearly showed that, when used as a single agent, AEE788 has potent antitumor and antiangiogenic activity

Table 2 Quantitative analysis of immunohistochemical staining of s.c. Colo16 tumors of nude mice treated with AEE788

Variable	Treatment group*	
	Control	AEE788
Tumor cells, mean ± SD		
PCNA (%)†	78.8 ± 6.2	26.3 ± 13.8‡
TUNEL (%)†	1.3 ± 0.8	12.1 ± 4.1‡
VEGF (absorbance)§	0.55 ± 0.03	0.64 ± 0.01‖
IL-8 (absorbance)§	0.50 ± 0.18	0.41 ± 0.19‖
bFGF (absorbance)§	0.80 ± 0.35	0.36 ± 0.20¶
Endothelial cells, mean ± SD		
MVD**	11 ± 3	4 ± 1‡
CD31/TUNEL (%)††	0	16.8 ± 8.2‡

*Colo16 cells (4×10^5) were injected s.c. into nude mice. Eleven days later, mice were randomized for treatment thrice weekly by oral gavage with either AEE788 (50 mg/kg) or the vehicle for AEE788 (control). Specimens were processed for immunohistochemical analyses 21 days after the start of treatment.

†PCNA and TUNEL positivity was quantitated as the ratio of positively stained cells to the total cells per field in 10 random 0.159-mm^2 fields at ×100 magnification.

‡$P < 0.001$ compared with controls (Student's t test).

§Absorbance determined as described in Materials and Methods.

‖$P > 0.05$ compared with controls (Student's t test).

¶$P < 0.01$ compared with controls (Student's t test).

**MVD was determined by measuring the number of completely stained blood vessels in 10 random 0.159-mm^2 fields at ×100 magnification.

††CD31/TUNEL positivity was quantitated as the ratio of CD31/TUNEL-positive cells to the total endothelial cells in each of 10 random 0.011-mm^2 fields at ×400 magnification.

against human cutaneous SCC growing in nude mice. In addition to inhibiting angiogenesis indirectly by blocking the EGFR signaling pathway, AEE788 directly inhibits VEGFR signaling pathway. Therefore, we suggest that treatment with AEE788 might exhibit a more potent antiangiogenic effect than would treatment with a selective anti-EGFR or anti-VEGFR agent, but further testing is needed to confirm this.

In summary, we have provided experimental evidence that blockade of the EGFR and VEGFR signaling pathways by the small molecule inhibitor AEE788 has significant therapeutic effects on human cutaneous SCC cell xenografts in nude mice. Therefore, the use of AEE788 may be a rational approach to the treatment of recurrent or metastatic cutaneous SCC and warrants further testing.

ACKNOWLEDGMENTS

We thank Dr. Isaiah J. Fidler (Department of Cancer Biology, University of Texas M.D. Anderson Cancer Center) for providing the Colo16 cell line and Dr. Gary L. Clayman (Department of Head and Neck Surgery, University of Texas M.D. Anderson Cancer Center) for providing the SRB1, SRB12, and HaCaT cells.

REFERENCES

1. Miller DL, Weinstock MA. Nonmelanoma skin cancer in the United States: incidence. J Am Acad Dermatol 1994;30:774–8.

2. Jemal A, Thomas A, Murray T, Thun M. Cancer statistics. CA Cancer J Clin 2002;52:23–47.

3. Albert MR, Weinstock MA. Keratinocyte carcinoma. CA Cancer J Clin 2003;53:292–302.

4. Budiyanto A, Bito T, Kunisada M, et al. Inhibition of the epidermal growth factor receptor suppresses telomerase activity in HSC-1 human cutaneous squamous cell carcinoma cells. J Invest Dermatol 2003; 121:1088–94.

5. Fujii K, Dousaka-Nakajima N, Imamura S. Epidermal growth factor enhancement of HSC-1 human cutaneous squamous cell carcinoma cell adhesion and migration on type I collagen involves selective up-regulation of $\alpha_2\beta_1$ integrin expression. Exp Cell Res 1995;216:261–72.

6. Shimizu T, Izumi H, Oga A, et al. Epidermal growth factor receptor overexpression and genetic aberrations in metastatic squamous-cell carcinoma of the skin. Dermatology 2001;202:203–6.

7. Ang KK, Andratschke NH, Milas L. Epidermal growth factor receptor and response of head-and-neck carcinoma to therapy. Int J Radiat Oncol Biol Phys 2004;58:959–65.

8. Esser S, Wolburg K, Wolburg H, et al. Vascular endothelial growth factor induces endothelial fenestrations *in vitro*. J Cell Biol 1998; 140:947–59.

9. Ferrara N, Houck K, Jakeman L, Leung DW. Molecular and biological properties of the vascular endothelial growth factor family of proteins. Endocr Rev 1992;13:18–32.

10. Elson DA, Ryan HE, Snow JW, Johnson R, Arbeit JM. Coordinate up-regulation of hypoxia inducible factor (HIF)-1 α and HIF-1 target genes during multi-stage epidermal carcinogenesis and wound healing. Cancer Res 2000;60:6189–95.

11. Larcher F, Robles AI, Duran H, et al. Up-regulation of vascular endothelial growth factor/vascular permeability factor in mouse skin carcinogenesis correlates with malignant progression state and activated H-ras expression levels. Cancer Res 1996;56:5391–6.

12. Maiolino P, De Vico G, Restucci B. Expression of vascular endothelial growth factor in basal cell tumours and in squamous cell carcinomas of canine skin. J Comp Pathol 2000;123:141–5.

13. Strieth S, Hartschuh W, Pilz L, Fusenig NE. Angiogenic switch occurs late in squamous cell carcinomas of human skin. Br J Cancer 2000;82:591–600.

14. Bowden J, Brennan PA, Umar T, Cronin A. Expression of vascular endothelial growth factor in basal cell carcinoma and cutaneous squamous cell carcinoma of the head and neck. J Cutan Pathol 2002;29:585–9.

15. Holsinger FC, Doan DD, Jasser SA, et al. Epidermal growth factor receptor blockade potentiates apoptosis mediated by paclitaxel and leads to prolonged survival in a murine model of oral cancer. Clin Cancer Res 2003;9:3183–9.

16. Magne N, Fischel JL, Dubreuil A, et al. Sequence-dependent effects of ZD1839 ("Iressa") in combination with cytotoxic treatment in human head and neck cancer. Br J Cancer 2002;86:819–27.

17. Myers JN, Holsinger FC, Bekele BN, et al. Targeted molecular therapy for oral cancer with epidermal growth factor receptor blockade. Arch Otolaryngol Head Neck Surg 2002;128:875–9.

18. Ang KK, Berkey BA, Tu X, et al. Impact of epidermal growth factor receptor expression on survival and pattern of relapse in patients with advanced head and neck carcinoma. Cancer Res 2002;62:7350–6.

19. Baselga J, Rischin D, Ranson M, et al. Phase I safety, pharmacokinetic, and pharmacodynamic trial of ZD1839, a selective oral epidermal growth factor receptor tyrosine kinase inhibitor, in patients with five selected solid tumor types. J Clin Oncol 2002;20: 4292–302.

20. Cohen EE, Rosen F, Stadler WM, Recant W. Phase II trial of ZD1839 in recurrent or metastatic squamous cell carcinoma of the head and neck. J Clin Oncol 2003;21:1980–7.

21. Herbst RS, Shin DM. Monoclonal antibodies to target epidermal growth factor receptor-positive tumors (a new paradigm for cancer therapy). Cancer 2002;94:1593–610.

22. Kedar D, Baker CH, Killion JJ, Dinney CPN, Fidler IJ. Blockade of the epidermal growth factor receptor signaling inhibits angiogenesis leading to regression of human renal cell carcinoma growing orthotopically in nude mice. Clin Cancer Res 2002;8:3592–600.

23. Hirata A, Ogawa S, Kometani T, et al. ZD1839 (Iressa) induces antiangiogenic effects through inhibition of epidermal growth factor receptor tyrosine kinase. Cancer Res 2002;62:2554–60.

24. Traxler P, Allegrini PR, Brandt R, et al. AEE788: a dual family epidermal growth factor receptor/ErbB2 and vascular endothelial growth factor receptor tyrosine kinase inhibitor with antitumor and antiangiogenic activity. Cancer Res 2004;64:4931–41.

25. Fan D, Poste G, O'Brian CA, et al. Chemosensitization of murine fibrosarcoma cells to drugs affected by the multidrug resistance phenotype by the antidepressant trazodone: an experimental model for the reversal of intrinsic drug resistance. Int J Oncol 1992;1:735–42.

26. Nicoletti I, Migliorati G, Pagliacci MC, Grignani F, Riccardi C. A rapid and simple method for measuring thymocyte apoptosis by propidium iodide staining and flow cytometry. J Immunol Methods 1991;139:271–9.

27. Lynch TJ, Bell DW, Sordella R, et al. Activating mutations in the epidermal growth factor receptor underlying responsiveness of non-small-cell lung cancer to gefitinib. N Engl J Med 2004;350:2129–39.

28. Uehara H, Kim SJ, Karashima T, et al. Effects of blocking platelet-derived growth factor-receptor signaling in a mouse model of experimental prostate cancer bone metastases. J Natl Cancer Inst 2003;95:458–70.

29. Yoneda J, Kuniyasu H, Crispens MA, et al. Expression of angiogenesis-related genes and progression of human ovarian carcinomas in nude mice. J Natl Cancer Inst 1998;90:447–54.

30. Craven RJ, Lightfoot H, Cance WG. A decade of tyrosine kinases: from gene discovery to therapeutics. Surg Oncol 2003;12:39–49.

31. Barnes CJ, Bagheri-Yarmand R, Mandal M, et al. Suppression of epidermal growth factor receptor, mitogen-activated protein kinase, and Pak1 pathway and invasiveness of human cutaneous squamous cancer cells by the tyrosine kinase inhibitor ZD1839 (Iressa). Mol Cancer Ther 2003;2:345–51.

32. del Peso L, Gonzalez-Garcia M, Page C, Herrera R, Nunez G. Interleukin-3-induced phosphorylation of BAD through the protein kinase Akt. Science 1997;278:687–9.

33. Sauter ER, Nesbit M, Watson JC, et al. Vascular endothelial growth factor is a marker of tumor invasion and metastasis in squamous cell carcinoma of the head and neck. Clin Cancer Res 1999;5:775–82.

34. Arbiser JL, Byers HR, Cohen C, Arbeit J. Altered basic fibroblast growth factor expression in common epidermal neoplasm: examination with *in situ* hybridization and immunohistochemistry. J Am Acad Dermatol 2000;42:973–7.

35. Neuchrist C, Quint C, Pammer A, Burian M. Vascular endothelial growth factor (VEGF) and microvessel density in squamous cell carcinomas of the larynx: an immunohistochemical study. Acta Otolaryngol 1999;119:732–8.

36. Obermair A, Kohlberger P, Bancher-Todesca D, et al. Influence of microvessel density and vascular permeability factor/vascular endothelial growth factor expression on prognosis in vulvar cancer. Gynecol Oncol 1996;63:204–9.

37. Bruns CJ, Solorzano CC, Harbiston MT, et al. Blockade of the epidermal growth factor receptor signaling by a novel tyrosine kinase inhibitor leads to apoptosis of endothelial cells and therapy of human pancreatic carcinoma. Cancer Res 2000;60:2926–35.

38. Kim SJ, Uehara H, Karashima T, et al. Blockade of epidermal growth factor receptor signaling in tumor cells and tumor-associated endothelial cells for therapy of androgen-independent human prostate cancer growing in the bone of nude mice. Clin Cancer Res 2003;9:1200–10.

39. Shaheen RM, Davis DW, Liu W, et al. Antiangiogenic therapy targeting the tyrosine kinase receptor for vascular endothelial growth factor receptor inhibits the growth of colon cancer liver metastasis and induces tumor and endothelial cell apoptosis. Cancer Res 1999;59:5412–6.

40. Baker CH, Kedar D, McCarty MF, et al. Blockade of epidermal growth factor receptor signaling on tumor cells and tumor-associated endothelial cells for therapy of human carcinomas. Am J Pathol 2002;161:929–38.

41. Goldman CK, Kim J, Wong WL, et al. Epidermal growth factor stimulates vascular endothelial growth factor production by human malignant glioma cells: a model of glioblastoma multiforme pathophysiology. Mol Biol Cell 1993;4:121–33.

42. Shiurba RA, Eng LF, Vogel H, et al. Epidermal growth factor receptor in meningiomas is expressed predominantly on endothelial cells. Cancer 1988;62:2139.

43. Solorzano CC, Baker CH, Tsan R, et al. Optimization for the blockade of the epidermal growth factor receptor signaling for therapy of human pancreatic carcinoma. Clin Cancer Res 2001;8:2563–72.

44. Weber KL, Doucet M, Price JE, et al. Blockade of epidermal growth factor receptor signaling leads to inhibition of renal cell carcinoma growth in the bone of nude mice. Cancer Res 2003;63:2940–7.

45. Nelson JM, Fry DW. Akt, MAPK (Erk1/2), and p38 act in concert to promote apoptosis in response to ErbB receptor family inhibition. J Biol Chem 2001;276:14842–7.

46. Pollack VA, Savage DM, Baker DA, et al. Inhibition of epidermal growth factor receptor-associated tyrosine phosphorylation in human carcinomas with CP-358,774: dynamics of receptor inhibition *in situ* and antitumor effects in athymic mice. J Pharmacol Exp Ther 1999;291:739–48.

47. Williams KJ, Telfer BA, Stratford IJ, et al. ZD1839 ("Iressa"), a specific oral epidermal growth factor receptor-tyrosine kinase inhibitor, potentiates radiotherapy in a human colorectal cancer xenograft model. Br J Cancer 2002;86:1157–61.

48. Park J, Park BB, Kim JY, et al. Gefitinib (ZD 1839) monotherapy as a salvage regimen for previously treated advanced non-small cell lung cancer. Clin Cancer Res 2004;10:4383–8.

49. Higgins B, Kolinsky K, Smith M, et al. Antitumor activity of erlotinib (OSI-774, Tarceva) alone or in combination in human non-small cell lung cancer tumor xenograft models. Anticancer Drugs 2004;15: 503–12.